

# Predicting Marfan Syndrome in Children With Congenital Ectopia Lentis: Development and Validation of a Nomogram

Kityee Ng<sup>1,\*</sup>, Bo Qu<sup>2,\*</sup>, Qianzhong Cao<sup>1</sup>, Zhenzhen Liu<sup>1</sup>, Dongwei Guo<sup>1</sup>, Charlotte Aimee Young<sup>3</sup>, Xinyu Zhang<sup>1</sup>, Danying Zheng<sup>1</sup>, and Guangming Jin<sup>1</sup>

<sup>1</sup> State Key Laboratory of Ophthalmology, Zhongshan Ophthalmic Center, Sun Yat-Sen University, Guangdong Provincial Key Laboratory of Ophthalmology and Visual Science, Guangdong Provincial Clinical Research Center for Ocular Diseases, Guangzhou, China

<sup>2</sup> Peking University Third Hospital, Beijing, China

<sup>3</sup> Department of Ophthalmology, Third Affiliated Hospital, Nanchang University, Nanchang, China

**Correspondence:** Danying Zheng, State Key Laboratory of Ophthalmology, Zhongshan Ophthalmic Center, Sun Yat-Sen University, Guangdong Provincial Key Laboratory of Ophthalmology and Visual Science, Guangdong Provincial Clinical Research Center for Ocular Diseases, Guangzhou 510060, China. e-mail: [zhengdy@163.com](mailto:zhengdy@163.com)

Guangming Jin, State Key Laboratory of Ophthalmology, Zhongshan Ophthalmic Center, Sun Yat-Sen University, Guangdong Provincial Key Laboratory of Ophthalmology and Visual Science, Guangdong Provincial Clinical Research Center for Ocular Diseases, Guangzhou 510060, China. e-mail: [jingm@mail2.sysu.edu.cn](mailto:jingm@mail2.sysu.edu.cn)

**Received:** May 12, 2023

**Accepted:** February 6, 2024

**Published:** March 19, 2024

**Keywords:** nomogram; marfan syndrome; prediction model

**Citation:** Ng K, Qu B, Cao Q, Liu Z, Guo D, Young CA, Zhang X, Zheng D, Jin G. Predicting marfan syndrome in children with congenital ectopia lentis: Development and validation of a nomogram. *Transl Vis Sci Technol.* 2024;13(3):15, <https://doi.org/10.1167/tvst.13.3.15>

**Purpose:** To derive an effective nomogram for predicting Marfan syndrome (MFS) in children with congenital ectopia lentis (CEL) using regularly collected data.

**Methods:** Diagnostic standards (Ghent nosology) and genetic test were applied in all patients with CEL to determine the presence or absence of MFS. Three potential MFS predictors were tested and chosen to build a prediction model using logistic regression. The predictive performance of the nomogram was validated internally through time-dependent receiver operating characteristic curves, calibration curves, and decision curve analysis.

**Results:** Eyes from 103 patients under 20 years old and with CEL were enrolled in this study. Z score of body mass index (odds ratio [OR] = 0.659; 95% confidence interval [CI], 0.453–0.958), corneal curvature radius (OR = 3.397; 95% CI, 1.829–6.307), and aortic root diameter (OR = 2.342; 95% CI, 1.403–3.911) were identified as predictors of MFS. The combination of the above predictors shows good predictive ability, as indicated by area under the curve of 0.889 (95% CI, 0.826–0.953). The calibration curves showed good agreement between the prediction of the nomogram and the actual observations. In addition, decision curve analysis showed that the nomogram was clinically useful and had better discriminatory power in identifying patients with MFS. For better individual prediction, an online MFS calculator was created.

**Conclusions:** The nomogram provides accurate and individualized prediction of MFS in children with CEL who cannot be identified with the Ghent criteria, enabling clinicians to personalize treatment plans and improve MFS outcomes.

**Translational Relevance:** The prediction model may help clinicians identify MFS in its early stages, which could reduce the likelihood of developing severe symptoms and improve MFS outcomes.

## Introduction

Marfan syndrome (MFS) is a severe systemic disease involving multiple organ systems including ocular, cardiovascular, and skeletal. Fibrillin-1 (FBN1) gene mutations are the primary cause of this condition.<sup>1</sup> Shockingly, there is a 1.1% mortality rate in children under 18 years old with MFS because of aortic disease,<sup>2,3</sup> and 26% of children with MFS will undergo at least one heart surgery.<sup>4</sup> Therefore early diagnosis and treatment are needed to delay the progression of clinical manifestations of MFS.

To date, the gold standard for the diagnosis of MFS is the revised Ghent criteria,<sup>5</sup> which was introduced 12 years ago. Aortic root dilation, ectopia lentis, high statures, arachnodactyly, and chest abnormalities are the most common clinical findings noted by physicians during physical examination and lead to suspicion of MFS.<sup>6</sup> Specifically, ectopia lentis was occurring in approximately 60% of MFS patients.<sup>2</sup> However, it is difficult to make a timely diagnosis of MFS even with the current, revised Ghent nosology, especially in children. Faivre et al.<sup>7</sup> studied 320 children with MFS and verified that the most of clinical manifestations of MFS developed with age. Moreover, ophthalmologists face significant challenges in distinguishing MFS from other conditions such as Weill–Marchesani syndrome and primary lens dislocation, because these conditions can present similar ocular manifestations of MFS. Chandra et al.<sup>8</sup> found that 46.3% of patients initially identified as having isolated ectopia lentis were later diagnosed with MFS based on the revised Ghent criteria after a 20-year observation period. This highlighted the inadequate applicability for differential diagnosis of MFS in children with ectopia lentis according to traditional criteria, and emphasized the importance of genetic testing as a diagnostic tool for MFS.<sup>9</sup> Nonetheless, genetic testing may introduce financial burdens to patients in developing countries or patients without means. Zhang et al.<sup>10</sup> pointed out that children and families in China tend not to accept outcomes of genetic testing because of a cultural stigma or lack of education around genetic diagnosis. The process of genetic testing can be associated with high costs and prolonged turnaround times. This makes it difficult to use genetic testing in the diagnosis of MFS. At present, several studies have tried to address the accuracy in predicting MFS.<sup>11,12</sup> Chen et al.<sup>11</sup> found axial length (AL)/corneal refractive power ratio could be a supplemental diagnostic predictor in MFS, whereas Sheikhzadeh et al.<sup>12</sup> suggested seven clinical variables to predict MFS. However, most studies in the field of screening MFS have only focused

on adults or have only focused on ocular parameters to identify MFS.

In this study, we intended to build a prediction model by combining the clinical data in the ocular, cardiovascular, and systemic systems together to differentiate MFS from other diseases among patients with congenital ectopia lentis (CEL). We hoped this prediction model could be used precisely and conveniently and thereby guide clinicians to optimize early diagnosis strategies of MFS from CEL patients.

## Methods

This study adhered to the tenets of the Declaration of Helsinki, and the Medical Ethics Committee of Zhongshan Ophthalmic Center of Sun Yat-Sen University approved this study. Informed consent in written form was obtained from all adult participants and the participants' guardians for those under 18 years old.

## Participants

A total of 103 patients with bilateral CEL who visited Zhongshan Ophthalmic Center from December 2018 to October 2021 were retrospectively reviewed. All cases of CEL patients were genetically confirmed as MFS or non-MFS.

All patients underwent a comprehensive systemic examination, including ocular system, cardiovascular system, and body mass index (BMI). Patients with traumatic lens history, uveitis, keratoconus, corneal disease, a history of ocular surgery, or use of contact lenses in the two weeks before the examinations were excluded from this study. Patients who were diagnosed with MFS according to Ghent II Nosology<sup>5</sup> and with genetic confirmation of the disease (confirmed heterozygous mutation FBN1) were eligible for the study. In total, among the 103 patients with bilateral CEL, 43 patients were identified as non-MFS group followed by the Ghent-2 diagnostic standard and genetic test and included four patients with ADAMTS gene mutation, one patient with CBS gene mutation, and two patients with LTBP2 gene mutation. For comparison, the non-MFS group was age- and sex-matched with the MFS group (Table 1).

## Ophthalmic Assessment

Board-certified ophthalmologists at the Zhongshan Ophthalmic Center examined the patients and subsequently divided them into two groups based

**Table 1.** Baseline Characteristics of Included Participants

	MFS	Non-MFS	P Value
Subjects/eyes	60/60	43/43	
Sex			
Female	14	31	
Male	27	31	
Age (years)	9.11 ± 3.63	9.39 ± 3.67	0.706
AL (mm)	24.13 ± 1.82	24.59 ± 2.15	0.290
CCR (mm/mm)	8.27 ± 0.37	8.05 ± 0.38	0.023
AL/CCR (mm/D)	2.98 ± 0.26	3.00 ± 0.21	0.762
CCT (mm)	562 ± 49.72	545 ± 63.92	0.604
WTW (mm)	13.26 ± 5.69	12.18 ± 0.47	0.030
Height (cm)	130.48 ± 17.19	125.57 ± 17.11	0.204
Weight (kg)	23.83 ± 8.68	28.75 ± 12.11	0.033
BMI	14.52 ± 2.58	15.69 ± 2.25	0.041
AO	24.21 ± 4.60	20.51 ± 3.64	0.001

CCT, central corneal thickness.

on the Ghent-2 criteria, followed by genetic testing. Medical and family histories were taken as well. All patients underwent slit-lamp examination after pupillary dilation to identify bilateral lens dislocation. Biometry was performed before any ocular treatment by using the IOLMaster 700 (Carl Zeiss Meditec, Jena, Germany) and pentacam HR (Oculus, Wetzlar, Germany). Biological parameters were collected, including keratometry (K), AL, white-to-white corneal diameter (WTW), and AL/corneal curvature radius (AL/CCR).

The z scores of AL, WTW, and CCR were all measured by using the following formula:  $Z\text{-AL} = (\text{measured AL} - \text{normative AL}) / \text{normative standard deviation (SD)}$ ;  $Z\text{-WTW} = (\text{measured WTW} - \text{normative WTW}) / \text{SD}$ ;  $Z\text{-CCR} = (\text{measured CCR} - \text{normative CCR}) / \text{SD}$ .<sup>13,14</sup> The normative ocular parameters were age and sex matched to normative peers' data published in the literature of Chinese population under 18 years old.<sup>15–17</sup> Thus a change in z score of 0 would indicate that a child has the same ocular growth and development rate compared to the age and sex matched peers, whereas an increase of the absolute value of z score would indicate that the value is above normal.

## Echocardiography

Patients with bilateral CEL were examined with a full ultrasound system (Philips EnVisor C-HD; Philips Co, Best, The Netherlands) by a qualified cardiac sonographer. The aortic root diameter was measured and compared to current guidelines.<sup>18</sup> Parasternal long-axis view was used to weigh up the aortic

measurements in three dimensions, including aortic annulus, sinotubular junction, and sinus of Valsalva. The aortic root diameter was measured as the largest diameter within the sinuses of Valsalva. Aortic Z-score was calculated in a website (<https://marfan.org/dx/zscore-children/#formtop>) by using the Colan formula, which followed the recommendations of the Marfan Foundation.

## Body Mass Index

The heights and weights were measured by nurses upon their first hospital visit. Participants were instructed before measurement of height and weight to only don light clothing. Measurements were taken using a portable stadiometer (Model S100; Ayrton Corp., Prior Lake, MN, USA) and a digital scale (Model 500KL; Health-oMeter, McCook, IL, USA). The BMI z score was calculated by BMI and transformed into age and sex-corresponding z score according to the World Health Organization's BMI for age growth charts.<sup>19</sup> The z-BMI is a relative BMI after adjusting for age and sex, compared with a reference standard, and was used because children naturally gain weight and height as they grow. Therefore it is necessary to adjust the BMI and compare with the same age and sex peers in the reference sample.

## Statistical Analysis

Continuous variables were reported in mean ± SD or median and interquartile ranges. Categorical variables were reported in integer and proportions. The

Kolmogorov-Smirnov test was applied for testing the normality of clinical variables. The one-way analysis of variance or Wilcoxon test was applied, as appropriate, to compare the continuous variables between two groups. The  $\chi^2$  test was applied for categorical variables.

The outcome measures in the present study were diagnosis of MFS (yes or no) in patients with CEL under 20 years old. Accordingly, logistic regression model was used for assessing the associations of relevant variables. The variables to be included in the multivariable logistic regression model were identified using a backwards stepwise selection method based on the Akaike information criterion. Variables with  $P < 0.05$  in the univariable models were incorporated into the multivariable logistic regression model. Selected variables were included in the nomogram to predict the diagnostic capability of MFS children by using statistical software (rms in R version 4.1.2, R Foundation). Calibration curves were used to verify the prediction model accuracy. A well-calibrated model shows that the predictions lie on a 45° diagonal line. The concordance index (C-index) and area under the receiver operating characteristic curve (AUC) were used to measure the predictive performance and discrimination ability of the nomogram. Generally, a C-index  $\geq 0.70$  represent a good estimation. The decision curve analysis was used to verify the clinical benefits and utility of the prediction model. The final model was internally validated by using 1000 bootstrap sampling procedure to calculate a C-index that incorporated relative correction. Statistical significance was reflected in  $P < 0.05$ . Statistical analyses were carried out with using Stata (version 16.0; Stata Corp, College Station, TX, USA) and R statistical software (R version 4.1.2, R Foundation).

## Results

### Clinical Characteristics of Participants

One hundred three eyes of 103 patients diagnosed with CEL were randomly selected in this study. Sixty patients were diagnosed with MFS (MFS group) and 43 patients were diagnosed with non-MFS (non-MFS group) by current Ghent-2 criteria and genetic screening. The mean age was  $9.11 \pm 3.63$  years old in MFS children compared with  $9.39 \pm 3.67$  years old in non-MFS children. Demographic factors and clinical features of two groups are listed in Table 1. There were no significant differences in the age, axial length, central corneal thickness, and AL/CCR ratio between the MFS and non-MFS groups ( $P = 0.706$ ,  $P = 0.290$ ,  $P = 0.604$ ,  $P = 0.762$ ).

Children in the MFS group had a flatter corneal, larger WTW compared with the non-Marfan group ( $P = 0.023$ ,  $P = 0.030$ ) in ocular features, whereas children in the MFS group had a lighter weight and smaller BMI compared with the non-MFS group in clinical features ( $P = 0.033$ ,  $P = 0.041$ ). According to echocardiography, the MFS group children had a larger AO value compared with the non-MFS group ( $P = 0.001$ ). These results are shown in Table 1.

### Z-Score Distribution

We found that when all the variables were transformed to Z-score, stronger correlations with the prediction model were obtained. Because there were no statistical differences in the z-CCR, z-BMI, and z-AO scores among different age groups ( $P = 0.548$ ,  $P = 0.745$ ,  $P = 0.816$ ) (Supplemental Fig. S1), the age difference can be well adjusted by the Z score. The distribution of CCR, BMI, and AO could be well represented by the Z-score (Fig. 1). In the MFS group, about 80% of MFS children had a smaller BMI with z-BMI score  $< 0$ , whereas half of non-MFS children had a normal BMI (Fig. 1A). Overall, 70.8% of MFS children had a flatter cornea (z-CCR  $\geq 1$ ), and 19.3% of patients had a prominent flatter cornea (z-CCR  $> 3$ ) (Fig. 1B), which large AO (z-AO score  $\geq 2$ ) was observed in 58% of MFS children (Fig. 1C).

The ocular, clinical, and cardiac features showing obvious differences were selected as potential prediction variables for the diagnostic model of MFS. Multiple logistic regression (Table 2) shown that z-CCR (odds ratio [OR] = 3.40, 95% confidence interval [CI], 1.83-6.31;  $P < 0.000$ ), z-BMI (OR = 0.66, 95% CI, 0.45-0.96;  $P = 0.029$ ), z-AO (OR = 2.34, 95% CI, 1.40-3.91;  $P = 0.001$ ) were significantly associated with development of MFS during childhood and adolescence.

### Nomogram and Model Performance

Three clinical variables (z-CCR, z-BMI and z-AO) were included as independent predictors for the nomogram (Table 2). Therefore a nomogram was established by using independent clinical variables to predict the MFS in childhood and adolescence (Fig. 2A). Total score based on the sum of the assigned number of points for each independent predictor in the nomogram was associated with the probability of diagnosis of MFS in childhood and adolescence. For example, if a total score of a patient is 110, their probability of MFS is 60%; therefore more attention should be paid to its subsequent development and follow-up. To make the predic-

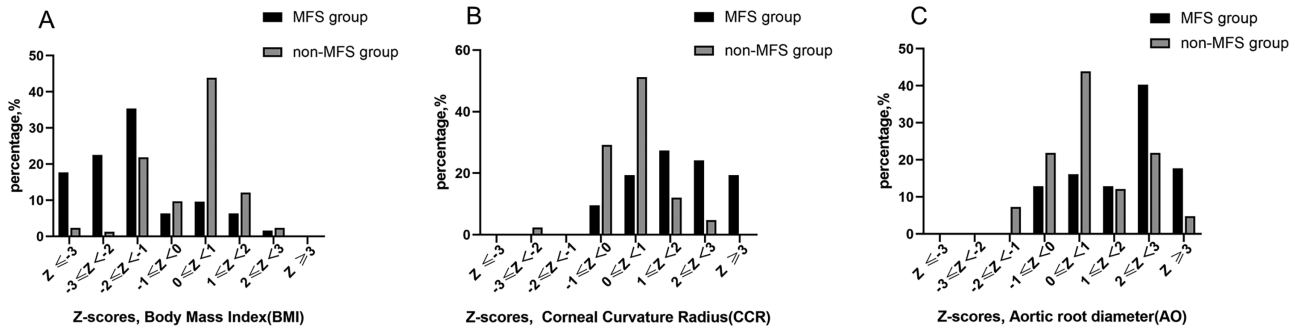


**Figure 1.** Analysis of z-score distribution of MFS and non-MFS patients. (A) Distribution of z-score of BMI in MFS and non-MFS patients. (B) Distribution of z-score of CCR in MFS and non-MFS patients. (C) Distribution of z-score of AO in MFS and non-MFS patients. .

**Table 2.** Potential Associated Factors of Marfan Syndrome

Variables	Univariable Analysis		Multivariable Analysis	
	OR (95% CI)	P Value	OR (95% CI)	P Value
Age (years)	0.98 (0.88–1.09)	0.703		
Sex	0.53 (0.23–1.17)	0.114		
z-BMI	0.53 (0.39–0.72)	<0.001	0.66 (0.45–0.96)	0.029
z-CCR	3.10 (1.90–5.04)	<0.001	3.40 (1.83–6.31)	<0.001
z-AO	2.54 (1.70–3.79)	<0.001	2.34 (1.40–3.91)	0.001
Weight	1.00 (0.97–1.03)	0.899		
BMI	0.99 (0.85–1.15)	0.899		
WTW	1.13 (0.80–1.59)	0.482		

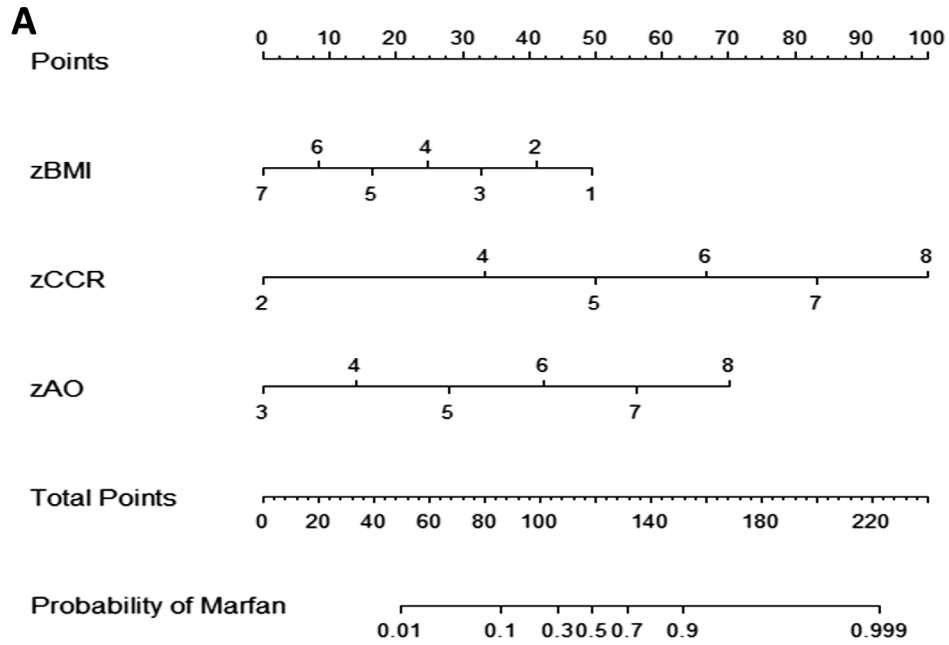
tive model more user-friendly and personalized for each clinician, an online MFS diagnostic calculator was further developed and is available online at the website (<https://ngkityee.shinyapps.io/DynNomapp/>), as screenshots in Figure 2B.

The bootstrap method was used to internally validate the resulting model. With an unadjusted C-index of 0.913 (0.861–0.965) and a bootstrap-corrected C-index of 0.902, the prediction model demonstrated good levels of accuracy for diagnosing MFS in CEL children. The calibration curves indicated an excellent agreement between prediction nomogram and observation (Fig. 3). The AUCs of the nomogram was 0.889 (95% CI, 0.826–0.953), which was better than each of the three predictors alone, including z-CCR (AUC = 0.731; 95% CI, 0.640–0.833), z-BMI (AUC = 0.740; 95% CI 0.636–0.845), z-AO (AUC = 0.754; 95% CI 0.654–0.855) (Fig. 4). This result suggested that the nomogram had a better level of discrimination for diagnosing MFS in CEL children. Once good discrimination and calibration were confirmed in the prediction model, its clinical benefit was evaluated. The decision curve analysis curves demonstrated that the nomogram can serve as an effective clinical approach and maximize the net clinical benefit (Fig. 5).

## Discussion

By identifying and analyzing the clinical risk factors of MFS patients, we can differentiate between the diagnosis of MFS with non-MFS in CEL patients. The prediction model demonstrates that, in combination with z-CCR, z-BMI, and z-AO, there may be a promising approach for the differentiation of MFS with high sensitivity (92.7%) and specificity (75.8%). Furthermore, this novel nomogram revealed a formula to calculate individual risk probability. This may help clinicians to screen for the disease based on baseline parameters to make individualized management strategies in a timely manner.

In this study, we found that CEL children with MFS generally had flatter corneas, which refers to a larger z-CCR, and the z-CCR was identified as a significant risk factor of MFS children. The association between cornea parameters and MFS patients was analyzed in previous studies.<sup>20–22</sup> Heur et al.<sup>23</sup> found that when compared to the normal patient, patients with MFS had smaller keratometry (K) values, and the K values could be served as a clinical diagnostic hallmark for MFS. However, longer AL often accom-



**B**  
Dynamic Nomogram

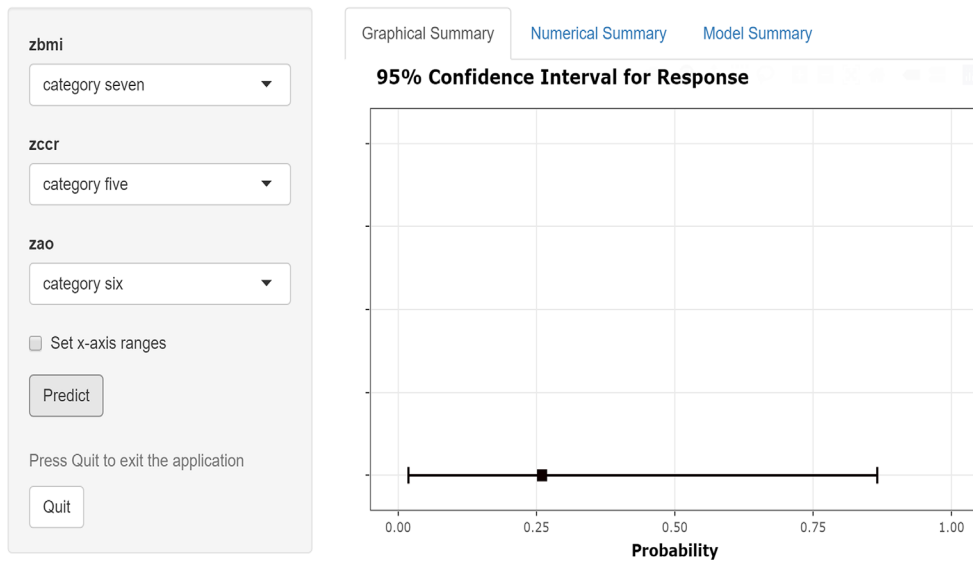


**Figure 2.** Nomogram for diagnostic probability in MFS using clinical factors. (A) This nomogram was based on three independent prognostic factors: z-BMI, z-CCR and z-AO. Point values can be identified from the points scale at the top of the nomogram. The sum of the point values for all existing prognostic factors results in the total points. Total points across the labelled scale can be read and correlated to the bottom scale, which provides the diagnostic probability of MFS. (B) Online dynamic nomogram for diagnostic probability in MFS accessible at the website <https://ngkityee.shinyapps.io/DynNomapp/>.

panies lower corneal power, even in healthy subjects,<sup>24</sup> which maintains equilibrium with the cornea’s hyperopic effect. In addition, when the confounding factor of axial length is eliminated, Luebke et al.<sup>25</sup> reported that the K value of MFS remains small and could serve as a screening tool for MFS suspects when compared

with healthy controls. The above findings are consistent with the present results that show patients with MFS have flatter corneas, and this can aid in distinguishing MFS from other diseases among CEL patients. Yet only one ocular parameter is used as the screening tool, which is not comprehensive and has not been

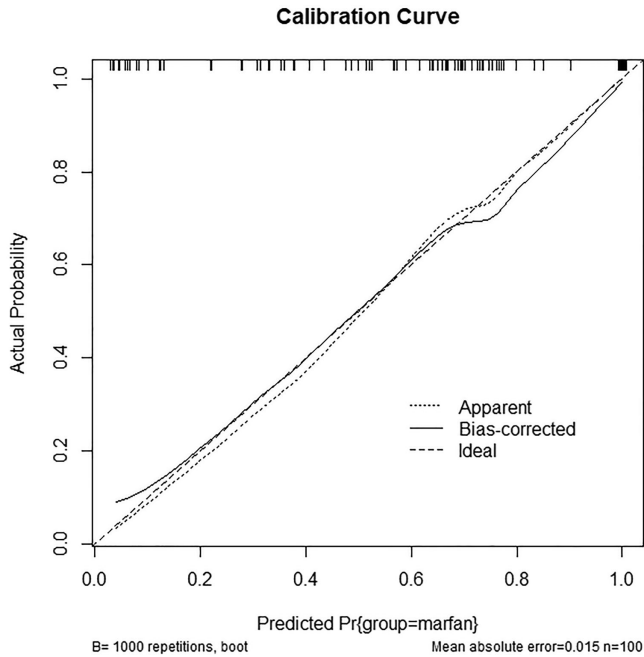


**Figure 3.** The calibration plot that compares the predicted and actual diagnostic probabilities. This shows good agreement with regards to the prediction of diagnosis of MFS between the risk estimation by nomogram confirmation.

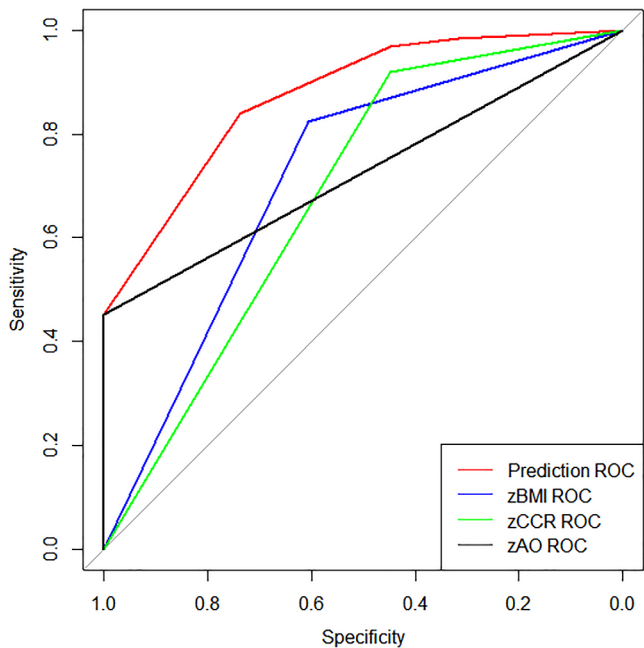


**Figure 4.** The ROC for predicting MFS with different predictor combinations showing AUC for the nomogram score (red line = prediction model with three predictors combined: AUC = 0.889; 95% CI, 0.826–0.953; green line = z-CCR: AUC 0.731, 95% CI, 0.640–0.833; blue line = z-BMI: AUC = 0.740, 95% CI, 0.636–0.845, black line = z-AO: AUC = 0.754; 95% CI, 0.654–0.855). ROC, receiver operating characteristic curves.

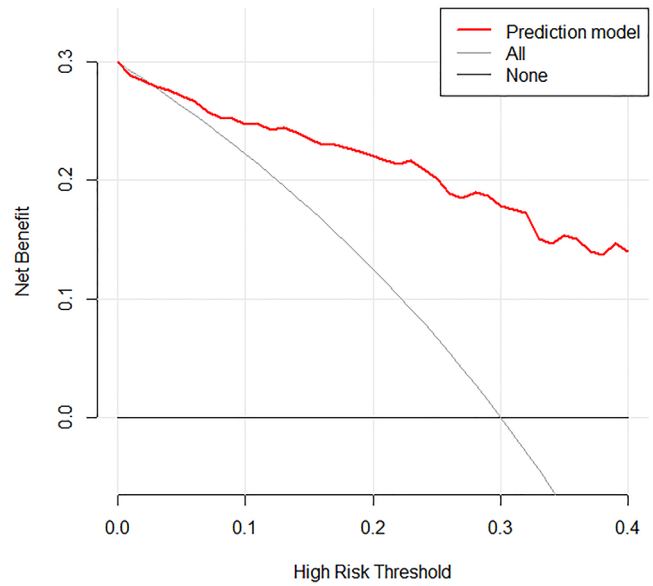


**Figure 5.** Decision curve analyses (DCA) for the nomogram. The x axis determines the threshold probability. The y axis determines the net benefit. The red line represents the MFS diagnostic nomogram. The gray line represents the assumption that all patients have MFS. The black line represents the assumption that patients without MFS. The decision curve indicated that the nomogram could obtain the maximum benefit in predicting MFS.

further evaluated and confirmed, especially in children. Because long AL and ectopia lentis can result by either FBN1 or ADAMTSL4 mutations.<sup>26</sup> It is important to compare the differences between MFS and non-MFS. In this study, we compared the ocular parameters of CEL patients with MFS and without MFS in children, which suggested that children with flatter corneas had a relatively high sensitivity.

We found that CEL children with MFS were thinner than children without MFS. MFS is often associated with a tall body stature.<sup>27</sup> Tall body stature is generally defined as a height above the 97th percentile or greater than 2 SD above the average height for age and gender in a defined population.<sup>28</sup> This feature can be one of the predictor of MFS. Stheneur et al.<sup>29</sup> reported that height could be a simple discriminating factor between MFS children and non-MFS children when the height >3.3 SD above the mean. On the contrary, we discovered that the height of MFS children was not statistically different from non-MFS children. Monteil et al.<sup>30</sup> postulated that height in MFS children was not a distinguishing trait, suggesting that children who grow faster in the non-MFS syndrome group could be attributed to being referred for suspected Marfan syndrome. Our study had more male participants in the non-MFS syndrome group, which may cause a referral bias from pediatricians and family

doctors, erroneously failing to refer female children whose characteristics may correspond to MFS. Second, the height was not corrected by age and sex factors, which may be attributed to the statistical insignificance. Furthermore, we use BMI ( $\text{kg}/\text{m}^2$ ) as a combination of weight and height, after adjusting the age and sex in terms of z-BMI. The study demonstrated that smaller BMI z scores in the MFS group compared with the non-MFS group significantly, indicating that BMI can be used to distinguish between the two groups.

Last, this study found the AO value of MFS children was larger than the non-MFS children among the CEL patients, and the z-AO is one of the predictors of MFS. This result was consistent with previous studies. It is well known that aortic root dilation is a major cardiac abnormality of MFS and is one of the most important diagnostic criteria. Because the diameter of the aortic root depends on the age, gender, and body surface area (BSA) of the patient. As a result, to determine whether the aortic root is dilated, a dedicated Z-score calculator should be used. An aortic root Z-score  $\geq 3$  is enough for a diagnosis of MFS if the patient is younger than 20 years of age.<sup>5</sup> Interestingly, our study found that only 9/62 patients who were diagnosed with MFS and the aortic root Z-score  $\geq 3$ . As a result, we have to combine the other predictors to construct a strong prediction model to distinguish MFS in CEL children.

So far, our model is built on the previous models, which has been refined and optimized. There were few options for a diagnostic predictive model capable of integrating multiple MFS risk factors. Sheikhzadeh et al.<sup>12</sup> proposed a risk score for MFS patients based on score points of existed signs such as ectopia lentis, wrist and thumb sign, family history of MFS, previous thoracic aortic surgery, skin striae, previous pneumothorax, and pectus excavatum. Chen et al.<sup>11</sup> reported an ocular diagnostic model based on the value of the axial length/total corneal refractive power ratio. In this study, we found that body stature, cardiac parameter, and ocular parameter (z-BMI, z-AO, z-CCR) contributed to the predictive factors. Our model has several advantages that should be considered. First of all, both of the existing models described above were developed in MFS adult patients with more severe clinical or developed manifestations, including previous history of relevant surgeries, whereas our study focused on MFS children with CEL, who require more attention in terms of treatment selection and prognosis. Second, we identified and adjusted three important and comprehensive predictors (z-BMI, z-AO, z-CCR) that were able to provide early, easy-to-obtain, and accurate prediction of MFS among CEL patients.

Third, we were able to rule out the confounding factors of age, and sex on MFS children because almost all MFS symptoms were progressive and age dependent. Our study must take into account certain limitations. First, the patient cohort was enrolled from a single ophthalmic center. Second, external validation is still needed in future longitudinal studies. Third, because of the fact that our study population primarily consisted of MFS patients under 18 years old, the applicability of the Ghent criteria may not be directly applicable to this subgroup. However, the development of this model still holds a certain level of necessity. Nonetheless, there are limitations to the generalizability of our model to MFS patients without CEL. Consequently, further studies with larger sample size and a longitudinal study would be required to validate our diagnostic predictive model and reach further conclusions.

In conclusion, we developed an optimized and individualized nomogram to provide accurate and early-stage diagnosis data for MFS children among CEL patients, a cohort of patients who require specialized clinical attention when it comes to their treatment strategies. This model has potential to assist in early intervention in an individual patient with progression of the disease. This tool may aid clinicians individualize management strategies of CEL patients with MFS.

## Acknowledgments

Supported by the National Natural Science Foundation of China (81873673, 81900841), and the Basic and Applied Basic Research Foundation of Guangdong Province (2021A1515011673, 2022A1515011181).

Disclosure: **K. Ng**, None; **B. Qu**, None; **Q. Cao**, None; **Z. Liu**, None; **D. Guo**, None; **C.A. Young**, None; **X. Zhang**, None; **D. Zheng**, None; **G. Jin**, None

\* KN and BQ are joint first authors.

## References

1. Dureau P. Pathophysiology of zonular diseases. 2008;19:27–30.
2. Bitterman AD, Sponseller PD. Marfan syndrome: a clinical update. *J Am Acad Orthop Surg*. 2017;25:603–609.
3. Daniel P, Judge M, Harry C, Dietz M. Marfan's syndrome. *Lancet*. 2005;366(9501):1965–1976.



4. van Karnebeek CD, Naeff MS, Mulder BJ, Hennekam RC, Offringa M. Natural history of cardiovascular manifestations in Marfan syndrome. *Arch Dis Child.* 2001;84:129–137.
5. Loeys BL, Dietz HC, Braverman AC, et al. The revised Ghent nosology for the Marfan syndrome. *J Med Genet.* 2010;47:476–485.
6. Wozniak-Mielczarek L, Osowicka M, Radtke-Lysek A, et al. How to distinguish Marfan syndrome from marfanoid habitus in a physical examination-comparison of external features in patients with Marfan syndrome and marfanoid habitus. *Int J Environ Res Public Health.* 2022;19:772.
7. Faivre L, Masurel-Paulet A, Collod-Bérout G, et al. Clinical and molecular study of 320 children with Marfan syndrome and related type I fibrillinopathies in a series of 1009 probands with pathogenic FBN1 mutations. *Pediatrics.* 2009;123:391–398.
8. Chandra A, Ekwalla V, Child A, Charteris D. Prevalence of ectopia lentis and retinal detachment in Marfan syndrome. *Acta Ophthalmol.* 2014;92:e82–83.
9. Bombardieri E, Rohrbach M, Greutmann M, et al. Marfan syndrome and related connective tissue disorders in the current era in Switzerland in 103 patients: medical and surgical management and impact of genetic testing. *Swiss Med Wkly.* 2020;150:w20189.
10. Zhang Y, Wang Z, Huang S, et al. Parents' perceptions of diagnostic genetic testing for children with inherited retinal disease in China. *Mol Genet Genomic Med.* 2019;7:e916.
11. Chen T, Chen J, Jin G, et al. Clinical ocular diagnostic model of Marfan syndrome in patients with congenital ectopia lentis by Pentacam AXL System. *Transl Vis Sci Technol.* 2021;10:3.
12. Sheikhzadeh S, Kusch ML, Rybczynski M, et al. A simple clinical model to estimate the probability of Marfan syndrome. *QJM.* 2012;105:527–535.
13. Martinez-Millana A, Hulst JM, Boon M, et al. Optimisation of children z-score calculation based on new statistical techniques. *PLoS One.* 2018;13:e0208362.
14. Chen ZX, Chen JH, Zhang M, et al. Analysis of axial length in young patients with Marfan syndrome and bilateral ectopia lentis by Z-scores. *Ophthalmic Res.* 2021;64:811–819.
15. Zhang YY, Jiang WJ, Teng ZE, et al. Corneal curvature radius and associated factors in Chinese children: the Shandong Children Eye Study. *PLoS One.* 2015;10:e0117481.
16. Lu TL, Wu JF, Ye X, et al. Axial length and associated factors in children: the Shandong Children Eye Study. *Ophthalmologica.* 2016;235:78–86.
17. Jiang WJ, Wu H, Wu JF, et al. Corneal diameter and associated parameters in Chinese children: the Shandong Children Eye Study. *Clin Exp Ophthalmol.* 2017;45:112–119.
18. Baumgartner H, Bonhoeffer P, De Groot NM, et al. ESC Guidelines for the management of grown-up congenital heart disease (new version 2010). *Eur Heart J.* 2010;31:2915–2957.
19. Bernal JL, Cummins S, Gasparrini A. Interrupted time series regression for the evaluation of public health interventions: a tutorial. *Int J Epidemiol.* 2017;46:348–355.
20. Suwal RCiAaCWMSFtMECoC,Khadka S, Joshi P. Ocular manifestations and biometrics in Marfan's syndrome from Eastern Nepal. *Clin Ophthalmol.* 2020;14:2463–2472.
21. Kinori M, Wehrli S, Kassem IS, Azar NF, Maumenee IH, Mets MB. Biometry characteristics in adults and children with marfan syndrome: from the marfan eye consortium of Chicago. *Am J Ophthalmol.* 2017;177:144–149.
22. Sultan G, Baudouin C, Auzeire O, De Saint Jean M, Goldschild M, Pisella PJ. Cornea in Marfan disease: Orbscan and in vivo confocal microscopy analysis. *Invest Ophthalmol Vis Sci.* 2002;43:1757–1764.
23. Heur M, Costin B, Crowe S, et al. The value of keratometry and central corneal thickness measurements in the clinical diagnosis of Marfan syndrome. *Am J Ophthalmol.* 2008;145:997–1001.
24. Fotedar R, Wang JJ, Burlutsky G, et al. Distribution of axial length and ocular biometry measured using partial coherence laser interferometry (IOL Master) in an older white population. *Ophthalmology.* 2010;117:417–423.
25. Luebke J, Boehringer D, Eberwein P, Reinhard T. Corneal K-values as a diagnostic screening tool for Marfan syndrome. *Cornea.* 2017;36:700–703.
26. Chandra A, Aragon-Martin JA, Hughes K, et al. A genotype-phenotype comparison of ADAMTSL4 and FBN1 in isolated ectopia lentis. *Invest Ophthalmol Vis Sci.* 2012;53:4889–4896.
27. Salim MA, Alpert BS. Sports and Marfan syndrome: awareness and early diagnosis can prevent sudden death. *Phys Sportsmed.* 2001;29:80–93.

28. Urakami T. Tall stature in children and adolescents. *Minerva Pediatr.* 2020;72:472–483.
29. Stheneur C, Tubach F, Jouneaux M, et al. Study of phenotype evolution during childhood in Marfan syndrome to improve clinical recognition. *Genet Med.* 2014;16:246–250.
30. Monteil DC, Shikany A, Aljeaid D, et al. Comparison of evolution of aortic root dilation and ghent criteria in preadolescents and adolescents with and without Marfan syndrome. *J Pediatr.* 2020;221:188–195.e181.